

ZhaoBin WANG
WeiYan LI
Shang SHANG
Zhan WANG
ChunYang HAN

PERFORMANCE DEGRADATION COMPARISONS AND FAILURE MECHANISM OF SILVER METAL OXIDE CONTACT MATERIALS IN RELAYS APPLICATION BY SIMULATION

PORÓWNANIE OBNIŻENIA CHARAKTERYSTYK ORAZ BADANIE MECHANIZMU USZKODZEŃ MATERIAŁÓW STYKOWYCH Z KOMPOZYTÓW TYPU SREBRO-TLENEK METALU STOSOWANYCH W PRZEKAŹNIKACH ELEKTROMAGNETYCZNYCH NA PODSTAWIE DANYCH Z SYMULACJI KOMPUTEROWEJ

To evaluate the electrical contact behaviors of silver metal oxide contact materials in relays application more accurately, and to guide the selection of contact materials, the test device and testing method for simulating electrical contact performance in relays application were analyzed in this paper. The electrical contact simulation test system was designed and developed, which can easily simulate contact materials. The contact resistance, static force and rebound energy degradation parameters of AgSnO₂, AgCdO and AgNi contact materials under the same load conditions were obtained through experimental research, the contact resistance and arcing energy degradation parameters of AgSnO₂ under different opening distances were acquired at the same time. The result indicated that accurate data are received by the electrical contact simulation testing method. Finally, based on the test data, the degradation performance of three selected test materials was tested, and the failure mechanism of AgSnO₂ materials was analyzed.

Keywords: electrical contact performance; contact material; degradation parameter; contact resistances; failure mechanism.

W celu dokładniejszej oceny zachowania styków elektrycznych z kompozytów srebra i tlenku metalu stosowanych w przełącznikach elektromagnetycznych oraz w celu ułatwienia wyboru materiałów stykowych, w niniejszej pracy przeanalizowano urządzenie testowe oraz metodę testowania, które pozwalają na symulację działania styku przełącznika. Zaprojektowano i zbudowano system testowania styków elektrycznych, który umożliwia łatwą symulację zachowania materiałów stykowych. Parametry degradacji rezystancji zestykowej, siły statycznej oraz energii odbicia materiałów stykowych AgSnO₂, AgCdO i AgNi uzyskano w badaniach eksperymentalnych prowadzonych w takich samych warunkach obciążenia. Jednocześnie badano także parametry degradacji rezystancji zestykowej energii łuku AgSnO₂ przy różnych odległościach otwarcia styków. Wyniki pokazują, że proponowana metoda badania symulacyjnego styków elektrycznych pozwala na uzyskanie dokładnych danych. W oparciu o dane testowe, przebadano zachowanie degradacyjne trzech wybranych materiałów oraz przeanalizowano mechanizm uszkodzenia styków z kompozytu AgSnO₂.

Słowa kluczowe: wydajność styku elektrycznego; materiał stykowy; parametr degradacji; rezystancja zestykowa; mechanizm uszkodzenia.

1. Introduction

The electrical properties of the contact material play a key role in the reliability of the automation system. Generally speaking, the performance indicators of the contact materials include contact resistance, resistance to fusion welding, corrosion resistance, hardness, strength and other related parameters [19]. Qualified contact materials should have good electrical and thermal conductivity, and should also have good mechanical, chemical, and arc-resistant properties as well [18]. In the working process of the contacts of the switch apparatus,

there are complex mechanical, electrical, thermal and arc energy conversions, so the traditional analysis method cannot effectively analyze the failure mechanism of low-voltage electrical appliances [10]. Because the silver-based contact material has good conductivity and thermal conductivity and has high oxidation resistance and small contact resistance, it is widely used in the field of low-voltage relays application [15]. AgSnO₂, AgCdO and AgNi composite contact materials are widely used for controlling products [9].

It is well known that the electrical life of a low-voltage switching devices is directly related to factors such as switching load conditions,

mechanical motion characteristics, working environment atmosphere, and contact material composition[2]. Therefore, the correspondence between the material composition of a single contact material and the electrical life of the switch is not deterministic. The characteristics of the variety of electrical types also require that we should discuss the relationship respectively among the arc of the contact material, the electrical contact performance and the electrical life of the switch. The relationship between the contact material and the electrical life of the switch has been drawing much attention from relay or material manufacturers. Therefore, choosing which kind of experimental simulation to fulfil an authentic and accurate evaluation has become a critical issue.

The contact fusion welding, excessive contact resistance and contact electrical erosion are three typical failure modes that occur during the electrical life test of relays [3]. The electric life test systems currently used can be classified into two types. One is to take the motor or exciter as the driving mode to simulate the contact pair splitting process [7]. Because the speed of the simulation is in the range of a few millimetres per second, the arc characteristic parameters can be captured during the test. If the strain force sensor is introduced, the welding force in the contact breaking process can be measured together [13]. Another method is to use the actual switch product as the carrier, perform electrical life test after assembling the contacts [11], and evaluate the performance of contact materials by testing the life of the switch [16].

If the motor with a slower speed is applied, the breaking speed of the contact can achieve in the hundreds of microns per second, so that the liquid bridge and its rupture process during the breaking of the contact pair can be observed [8]. The electromagnetic coils and lever structures have been used to drive the contact pairs to split and close motion [3], and the simulated speed is within the range of 100 ~ 600 mm/s [1]. Moreover, piezoelectric force sensors are used to test the welding force of the contact, to evaluate the anti-welding performance of the contact materials [5]. Taking the electromagnetic relay as an example, the contact breaking process has a variable acceleration motion characteristic, with the maximum speed order of several hundred millimetres per second.

Compared with the actual relay, there are still some differences between the previous simulation test system and the actual relay, which are mainly reflected in the following aspects: (1) it is impossible to obtain the influence of the process adjustment parameters (magnetic clearance, contact opening distance, mechanical reaction force, static force, etc.) specifically to electrical switches on dynamic characteristics and the welding force; (2) with the limitation of the response speed of the force sensor, the movement form and breaking speed of the contact in the simulated action process are different from the actual electrical contact action process. So the conclusions obtained cannot be directly applied to the optimization of structural parameters and the selection of contact materials of the actual relays.

In this article, we present the test device and testing method for simulating electrical contact behaviour in relays application. The test system was designed in this paper using a typical clapper electromagnetic relay as the contact material test carrier, and a multi-degree-of-freedom joint mechanical adjustment mechanism was designed to realize the relay magnetic gap and contact opening distance, mechanical reaction force, static force adjustable function. During the relay action, the contact static force, welding force, collision force, contact dynamic displacement/speed, coil current, contact arc voltage/arc current, and related time parameters [17] can be measured simultaneously. It can also synchronously test the collision, rebound and fusion welding at the contacts during the relay pull-in/release process. In this paper, AgSnO₂, AgCdO and AgNi contact materials are taken as the research objects, and the electrical contact simulation test system of contact materials is designed. The degradation of electrical contact characteristic parameters of three kinds of materials under the same

load was compared, and the degradation of electrical performance parameters of AgSnO₂ at different opening distance was compared in the experiment. The variation of sensitive characteristic parameters of its electrical contact performance was analyzed, and its failure mechanism was preliminarily analyzed.

2. Novel test system for simulating and evaluating electrical contact characteristics of contact materials

At the present stage, there are two main ways to establish the electrical contact simulation test system for the contact materials: a) Using the electromagnetic coil or the exciter as the driving mechanism, simulating the breaking and closing process of the contact switch, and obtaining the contact welding force, etc. [6]; b) The actual switch product is used as the test carrier, and the switch apparatus is placed in the test system to test the arc characteristics and anti-welding characteristics of the switch apparatus [12]. Although the latter method can make a real analysis of the action characteristics of the actual electrical apparatus, it is limited by the structure of the electrical apparatus themselves, so it is impossible to change the mechanical parameters and accurately observe the erosion condition of the surface of the electrical equipment. In this test system, the electromagnet coil is used to drive the pushrod to act on the moving reed, and the dynamic and static contact points are used to simulate the on-off process of the electrical switch.

2.1. Main functions and technical indicators

Main functions: The system can change contact materials which were processed into rivet shapes freely to carry out electrical contact simulation test; adjust the mechanical parameters arbitrarily, including contact opening distance, pushrod position, empty travel (free travel of pusher) and super-path, etc., to assist in obtaining high-precision test data; real-time monitoring of the contact voltage, contact current, contact voltage drop and force signal in each switching/closing process; the static force, contact resistance, arc energy (breaking arc energy), rebound energy (closing arc energy) and relevant time parameters in each operation process were calculated according to the comprehensive electrical performance parameter program.

Technical index: contact voltage measurement range 0~48 V under DC condition, contact voltage accuracy 10 mV; contact current measurement range 0~20 A, contact current accuracy 10 mA; mechanical parameter adjustment mechanism adjustment accuracy 10 μm; contact resistance accuracy 0.1 mΩ; the time parameter accuracy is 1 μs.

2.2. Test system overall structure

The functional block diagram of the contact material electrical contact test system is shown in Fig. 1. The system is mainly divided into three parts: the mechanical system part, which realizes the dynamic adjustment of the mechanical parameters; the control conditioning part, including the action control module, electromagnet driving circuit, and the signal Conditioning acquisition module, to realize the drive control electromagnet action, amplify, filter and process the collected signals; the system software part uses Labview software to design the human-computer interaction interface, which can complete the functions of setting test parameters, test control, waveform display, and data management. The major structures and physical map of the test system are shown in Fig. 2.

In Fig. 2 the contact voltage and the contact voltage drop in the process of breaking and closing are respectively tested by the resistance voltage division method and the differential amplifier, the contact current is monitored by the Hall current sensor, the static force between the contacts is monitored by the force sensor, and the contact resistance is tested by the four-wire method. The original data

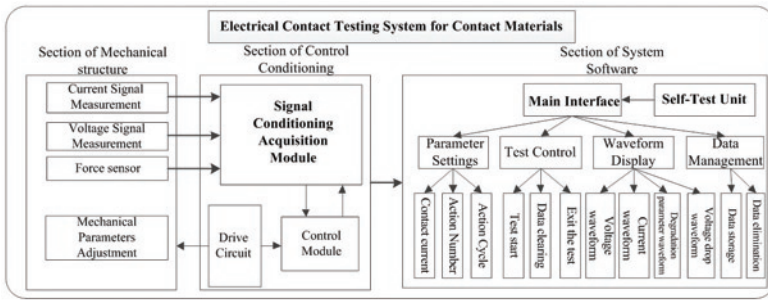
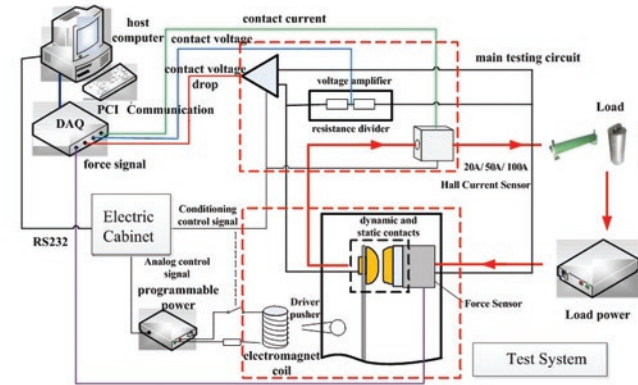


Fig. 1. Functional block diagram of the testing system for contact materials



a) Main structure of the test system

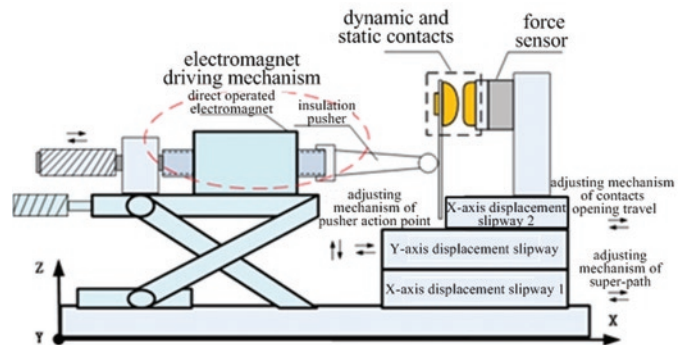
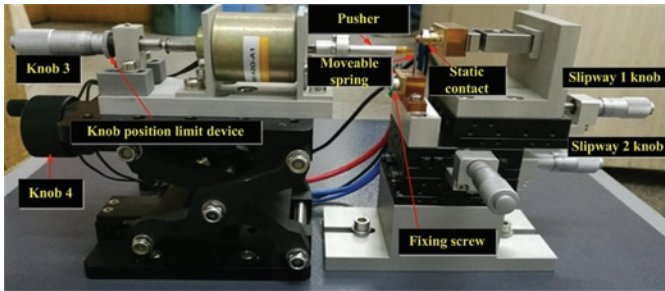


Fig. 3. Structural block diagram of mechanical system



b) physical map of the test mechanical system

Fig. 2. The major structures and physical map of the test system

collected by DAQ (Data Acquisition) are sent to the upper computer through the PCI (Peripheral Component Interconnect) communication protocol, and the upper computer communicates with the lower computer through the RS232 interface to complete functions such as comprehensive parameters dynamic observation and data storage of the electrical performance simulation test. If the contact appears adhesion failure, it will prompt the tester to stop the test system and cut off the load circuit.

2.3. Mechanical structure of the test system

Mechanical structure of the simulation test system includes electromagnet drive mechanism, lifting platform, horizontal sliding table, electromagnet stroke adjustment mechanism (empty travel), pushrod point adjustment mechanism, contact opening distance adjustment mechanism, hall current sensor and static force sensor, combined with the corresponding connector to achieve the adjustment of mechanical adjustment parameters, etc. The mechanical structure is shown in Fig. 3.

The front end of the direct-acting electromagnet of the system is fixed with an insulating pushrod for simulating the movement of the electric switch pushrod, and the left side is an electromagnet stroke adjusting mechanism, and the stroke of the electromagnet can be adjusted by adjusting the differential probe. The driving mechanism and

the adjusting mechanism are fixed on the Z-axis displacement slide, which can adjust the action point of the putter in the Z-axis direction of the moving reed. The dynamic and static contacts are respectively riveted on the moving reed and the static contact seat, the moving reed is fixed on the two-dimensional slide table, and the static contact seat is fixed on the two-dimensional sliding platform through the X-axis displacement sliding platform 2, the mechanical system can adjust the action point of the push rod on the Y-axis direction of the moving reed by adjusting the Y-axis displacement slide, adjust the over-travel by adjusting the X-axis displacement slide 1, and adjust the contact separation by adjusting the X-axis displacement slide 2. Adjustment of the opening distance. A static force sensor is fixed behind the static con-

tact seat, which can detect the static force signal of the contact.

3. Contact material performance comparison test and result analysis

3.1. Experimental test conditions

Three kinds of contact materials of $AgSnO_2$, $AgNi$ and $AgCdO$ were tested under the same condition. The contact test material electrical contact simulation test conditions and general composition of materials under test were shown in Table 1. The data obtained from the test were analyzed, and the variation trend curves of degra-

Table 1. Electrical contact simulation test conditions for contact materials

| Test parameters | Value |
|-------------------------|--|
| Experiment environment | Room temperature: 19°C~ 22°C; Humidity: 50 ~ 65% |
| Contact material | $AgSnO_2$, $AgNi$, $AgCdO$ |
| Operating frequency | 1s on/1s off |
| Load characteristics | Pure resistive load, full process is charged |
| Contact voltage/current | 24V/18A |
| Action number | Set continuous actions 20,000 times |
| Contact opening range | 0.6mm, 0.8mm |
| Initial static force | 1.5N |

dation parameters (contact resistance, static force, rebound energy) of the three materials were obtained by using the mean value method.

3.2. Experimental test result and analysis

3.2.1. Contact resistance

It is generally believed that the value of the contact resistance

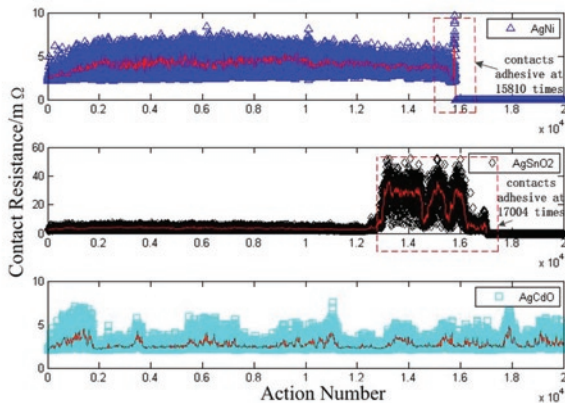


Fig. 4. Comparison of contact resistance change

depends on the resistivity, hardness, contact force and surface finish of as well as the chemical stability of the material, the magnitude of the current, conduction time, working environment and other factors [14]. In our test equipment and test conditions, the average contact resistance of AgSnO_2 , AgNi , and AgCdO were $7.7\text{m}\Omega$, $4.03\text{m}\Omega$ and $2.74\text{m}\Omega$ respectively.

It can be seen from Fig. 4 that the contact resistance of the Ag-SnO_2 contact material tends to be stable 13,000 times before, after a sharp increase in $50\text{m}\Omega$ situation, then the contact resistance began to fluctuate and decrease until the adhesive failure occurred at the 17004th time. In the early stage of the test, AgSnO_2 material has low and stable contact resistance due to arc erosion, which is not serious. With the increase of switching operations, the local molten pool will be formed on the surface of AgSnO_2 material under the impact of large current and arc erosion. As SnO_2 particles are hardpoints, they have good thermal stability, so no decomposition or sublimation occurs. Most of the SnO_2 particles have a lower density than the molten Ag , which will be suspended in the molten pool and form a SnO_2 particle aggregation area on the surface of the contact, resulting in increased contact resistance. In the later stage, due to the repeated thermal action of the arc, the surface topography between the contacts changes strongly, resulting in the softening of materials, the increase of metal bridge points in the fusion welding, part of the conductive spots no longer conduct electricity, and the fluctuation of contact resistance decreases until the bonding.

The contact resistance of AgCdO contact material always fluctuates around $2.5\text{m}\Omega$. As silver and cadmium oxide are not mutually soluble, CdO will decompose and absorb a large amount of heat under the action of arc. A part of the decomposed Cd will re-form CdO with the oxygen in the air on the surface of contact, hindering the fusion welding of moving and static contact. The contact surface of AgCdO has uniform erosion, low contact resistance, and good stability, and its resistance to fusion welding is the best.

For AgNi contact materials, under the action of 18A current, with the increase of switching operations, the erosion between dynamic and static contacts is serious and the material quality changes significantly. The pollution area increases and the contact resistance suddenly increases and a short adhesive failure occurs after 15810th time.

3.2.2. Static force

Fig.5 shows the static force test of three kinds of contact materials. The initial static force of the contact is set to 1.5N (We chose a pressure of 1.5N because the contact pressure of a certain sealed relay we analyzed was 1.5N. The test conditions are consistent with the actual relay product.). The arc of initial breaking process may belong to the anode (static contact) and the energy is high, causing the material of the initial closed contact surface to be transferred sharply. The surface of the cathode (moving contact) will have a certain convex dome, and the convex pressing of the static contact causes the interaction force between the two contacts to change, so the static force of three kinds of material maintained an upward trend at the beginning of the test. With the increase of the moving action of the moving and static contacts, the material of the contact surface accumulates, the transfer rate of the surface material slows down, and the steady trend is maintained for a long period time in the medium term.

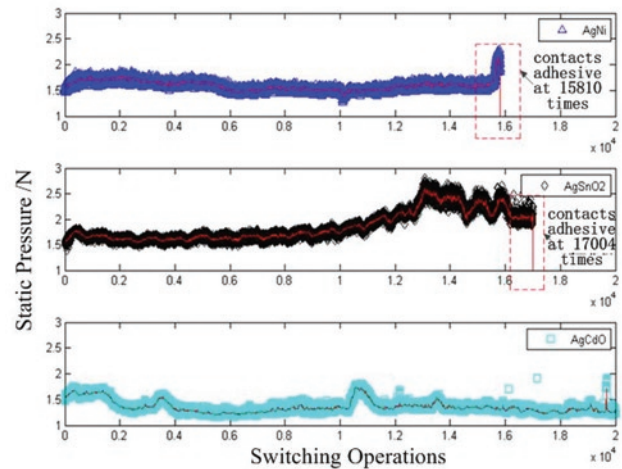


Fig. 5. Comparison of rebound energy change

In our test conditions and test equipment, the static force of the AgNi , AgSnO_2 contact materials fluctuate a lot before the contact fusion failure occurs, and achieve a higher value of about 2.3N, 2.8N, respectively. This may indicate that the material transfer is large and the arc erosion is serious, dynamic contact surface microscopic spikes occurred plastic deformation, the mechanical breaking strength is not enough to make it separated, cause adhesive failure of the contact. While the static force of AgCdO increased first and then fluctuated around 1.55N all the time, and the rise of temperature was low and it's not easy to weld. Therefore, the change of static force may be directly related to the surface morphology and microstructure of the contact.

3.2.3. Rebound energy

The rebound energy (closing arc energy) and the arc energy (breaking arc energy) which are in Fig.6 and Fig.8 can be calculated from the same formula as follow:

$$Q = \int_{t_0}^{t_1} u i dt = \sum_{i=1}^n U_i I_i \Delta t \quad (3)$$

Formulas:

- t_0 - the arcing start time (rebound start time);
- t_1 - the arcing end time (rebound end time);
- U - the contact voltage;
- I - the contact current;
- Δt - $4\mu\text{s}$ in our test system (corresponds to the sampling time)
- n - $(t_1 - t_0) / \Delta t$

It can be seen from Fig. 6 that the rebound energy of the three materials is maintained at 50mJ~130mJ for most of the time, and there is a tendency to decrease at the initial stage. The reason may be that the increase of static force suppresses the vibration of the contact closure process, while the possible reason for the increase of the rebound energy before the adhesive failure of the AgSnO₂ contact material is the increase of the contact return time, the number of rebounds and more frequent vibration. For the AgNi and AgSnO₂ materials, the welding phenomenon hinders the breaking of the contacts when the bonding failure occurs, and the rebound of the contacts is suppressed to some extent, and the rebound energy shows a sharp decline trend. During the test, the rebound energy of AgCdO material kept a small fluctuation around 85mJ, and the number of contact rebounds and rebound time were relatively stable.

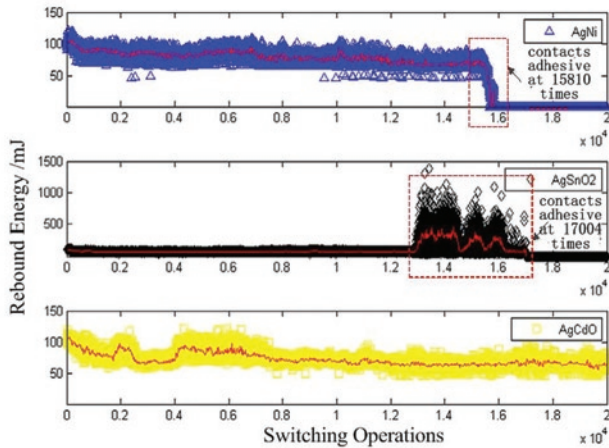


Fig. 6. Comparison of rebound energy change

Through the comparative analysis of the contact resistance, static force and rebound energy of the three materials mentioned above, it can be seen that AgSnO₂ has better resistance to fusion welding than AgNi, but its temperature rises higher, so adhesion is easy to occur under continuous action, and the contact resistance is higher than those of AgNi and AgCdO. AgNi contact material has poor welding resistance under slightly higher current conditions, but it has excellent processing performance with low cost, which is generally applicable to low voltage and small current microswitch appliances. In our test conditions and test device, AgCdO has better stability and strong resistance to arc ablation. However, under the continuous action of high-temperature arc, CdO will decompose Cd which is harmful to human body, so it is gradually replaced by other electric materials. The arc erosion mechanisms of the three materials are different. AgNi is the dissolution and precipitation effect derived from the metallurgical effect, while AgSnO₂ and AgCdO are mainly determined by the surface kinetics characteristics. In the following study, the surface morphology characteristics after material erosion will be observed through a microscope to further investigate.

4. Analysis of influence of opening distance on contact characteristics of contact materials

In our test equipment and test conditions, in order to study the influence of opening distance on the parameters of contact materials, AgSnO₂ material was taken as an example to make a comparative analysis on the parameters of contact resistance, arc ignition energy, arc ignition time and rebound energy under two opening distances. Because of the limited time, the relevant tests were only repeated three times, and the trend was the same. In future research work, we

will continue to test and analyze the results of the experiments and the thermal effects will be considered in the future publications.

4.1. Measured results of contact resistance at two opening distances

The experimental results of contact resistance at two opening distances are shown in Fig.7.

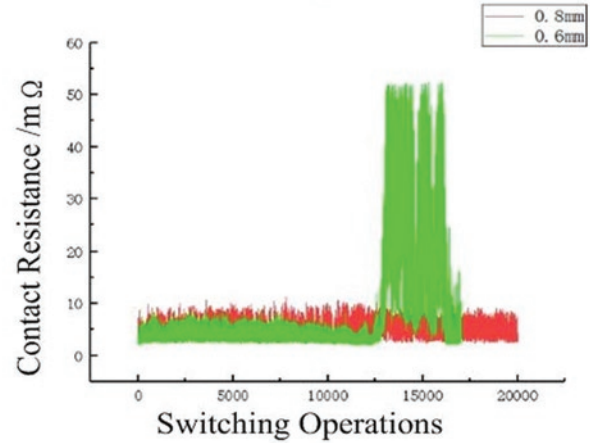


Fig. 7. Contact resistance comparison of AgSnO₂ at two opening distances

Under the two opening distance conditions, the contact resistance is kept at a low level in the first and middle stages of the operation, no more than 10mΩ. In the case of an opening distance of 0.6mm, the contact resistance begins to decrease at approximately 10,000 operations. There is no significant change in the contact resistance at the 0.8mm opening distance.

4.2. Measured results of arc time and arc energy at two opening distances

The measured results of arc time (the time between first and last arc) and arc energy at two opening distances are shown in Fig.8 and Fig.9.

The waveform of arc time and arc energy are very similar. The arc energy and arc time at 0.8mm opening distance are close to the data of 0.6mm opening distance before the 1000th movements. After the 1000th movements, the arc energy and arc time are kept low at 0.8mm opening distance. The arc energy is around 100~300mJ. At the same time, after the 12,000th movements, a strong arc of more than 2000mJ begins to appear, and the frequency of strong arc increases gradually.

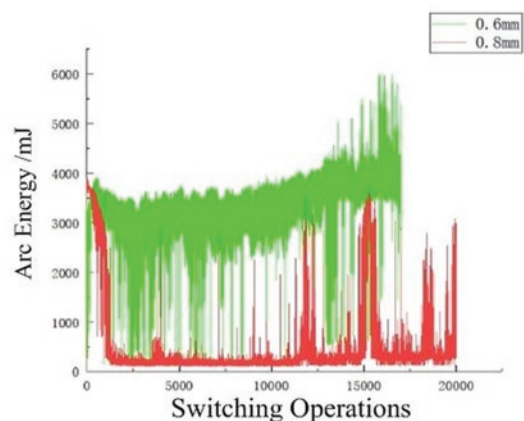


Fig. 8. Arc energy comparison of AgSnO₂ at two opening distances

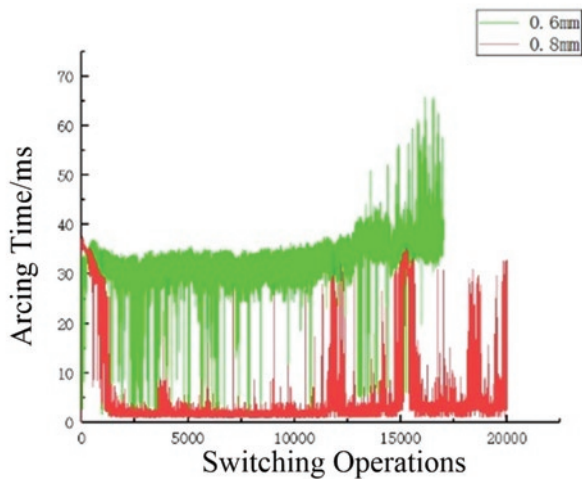


Fig. 9. Arc time comparison of AgSnO_2 at two opening distances

4.3. Measured results of rebound energy at two opening distance

The measured results of rebound energy at two opening distance are shown in Fig.10.

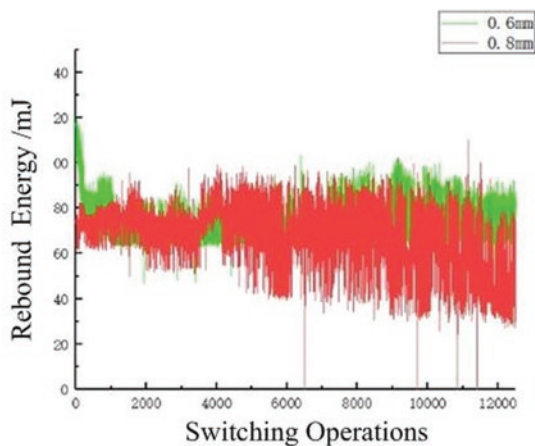


Fig. 10. Rebound energy comparison of AgSnO_2 at two opening distances

In the case of the opening distance $d=0.6\text{mm}$ and $d=0.8\text{mm}$ under our test equipment, the mean value of the rebound energy of the contact is roughly equal, and the fluctuation of the rebound energy under the opening distance of 0.8mm is more severe. The larger the contact opening distance, the greater the initial breaking force that the contact can achieve, which enhances the ability of the contact to break the weak adhesion. At the same time, the greater the breaking force is, the greater the breaking speed of the contacts will be, which is also conducive to the extinguishing of the arc.

5. Failure process analysis of AgSnO_2

In the electrical life simulation experiment, the contact resistance and static force of AgSnO_2 at 0.6mm spacing are shown in Fig. 11. At the beginning of the contact working process, the contact surface is relatively pure, so under the heat generated by the arc, the material transfer and pollution on the contact surface are more severe, which cause the surface morphology of rapid change, and the layer of oxides carbides (It is mainly oxides, but sometimes we can also detect the carbides. Perhaps it is related to the experimental atmosphere.) is accumulated on the contact surface, making the static force rise rapidly

at the beginning of the work, increase from 1.4N to approximately 1.8N . Then the upward trend of static force was restrained and began to show cyclical fluctuations.

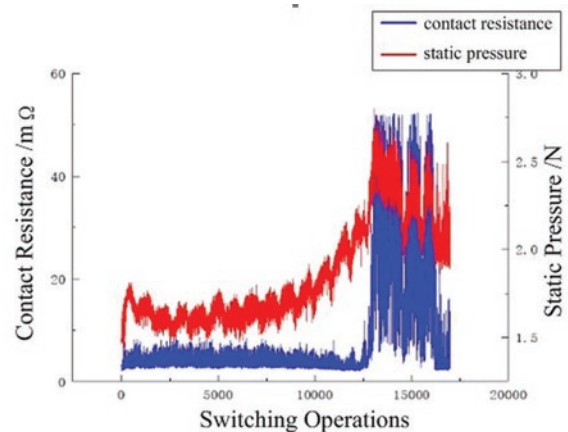


Fig. 11. Comparison of contact resistance and static force of AgSnO_2

According to the comparison between the contact resistance and the static force in some periods in Fig. 12, it can be found that the periodic fluctuation of the contact resistance and the static force are inversely proportional. This is because the high temperature generated by the arc causes the carbides formed on the surface to disappear during the material transfer, the contact material has a certain softening or even melting, and formed some relatively raised metal spike as the contact breaking, which reduces the actual contact area between the contacts, reduces the static force, and makes the contact resistance rise. After that, with the erosion of the arc and spatter of the material, the surface material of the contact produces loss, and some of the sharp peaks are re-worn, the actual distance between the contacts increases to the previous level, and the static force of the contact increases and while the contact resistance decreases. In the later stage of the test, with the erosion of the arc, the process mentioned above is repeated, and the contact material is continuously eroded in this process, resulting in material transfer and material loss.

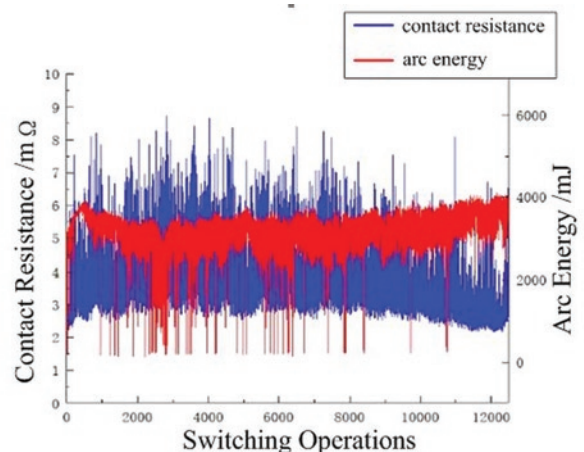


Fig. 12. Arc time comparison of AgSnO_2 at two opening distances

According to the contrast of contact resistance and arc energy of AgSnO_2 after 12000 actions in Fig. 12, the surface morphology of the contacts constantly changes and the relatively convex peaks increase due to the high temperature generated by the continuous arc, which make actual contact area between the contacts are gradually restored to the original level. Therefore, after the initial rising trend of contact resistance, it begins to decline to the initial level, and the contact re-

sistance fluctuates very sharply in this process. As the amount of contact arc erosion, the moving contact has a large range of ridges due to material transfer, and the static contact causes additional loss due to splashing in the process of material transfer, thus it will lead to the actual distance between the contacts increases, which will aggravate the rebound phenomenon when the contacts are closed. At the same time, the metal bridge occurs between the contacts due to the welding phenomenon during the working process, which makes contact separation need larger breaking force. The static force also becomes larger, which suppresses the rebound of the contacts. The final effect of these two aspects acting on the working process of the contact at the same time is shown in Fig.13 and Fig.14.

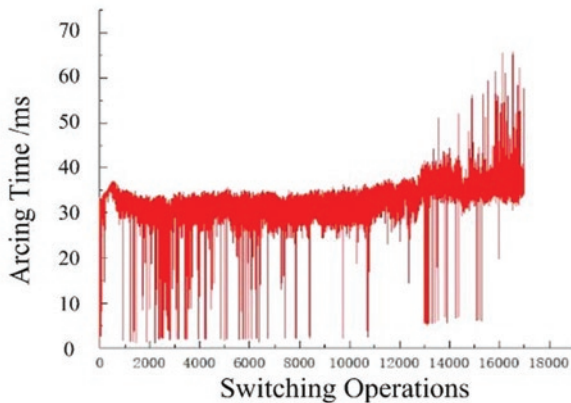


Fig. 13. Arc Burning Time of $AgSnO_2$

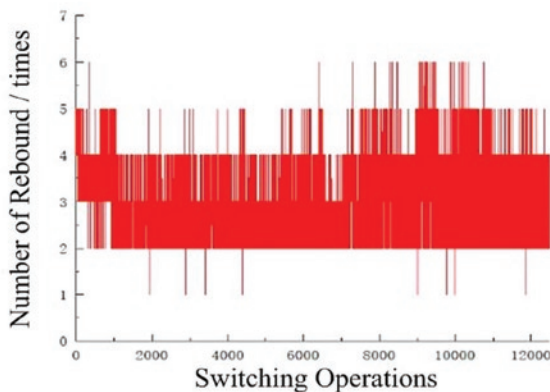


Fig. 14. Arc energy comparison of $AgSnO_2$ at two opening distances

It can be seen from the figure that, on one hand, the arc time and the arc energy increase when the contact is released, which obviously

increases the amount of contact arc corrosion. On the other hand, the rebound phenomenon of the contact is slightly increased, and the frequency of 4, 5 times or even 6 times jumps increases. All these changes will aggravate contact erosion, and as this process continues, the loss of contact materials will become more and more serious, and finally there will be obvious abnormalities in its electrical properties, leading to complete wear and failure of the metal layer of contact materials.

6. Conclusion

- (1) (1) An electromagnet push-rod type contact material test system is designed to simulate the action of relays. This system can analyze the influence of different contact materials, different load levels and different mechanical parameters on the electrical properties of the contact materials.
- (2) By comparing the electrical properties of $AgSnO_2$ at different opening distance, the relationship between contact opening distance and electrical properties of contacts was preliminarily analyzed. It was verified that larger contact opening distance can reduce arc erosion and overcome the welding force, thus helping to extend contact life;
- (3) Through the analysis of the degradation trend of electrical performance parameters during the test of $AgSnO_2$ materials, the failure mechanism is analyzed. The material mass transfer and loss caused by arc erosion, mechanical wear and other factors are the main reasons of the contact failure of the $AgSnO_2$ materials. The contact gradually develops a fusion phenomenon due to the high temperature generated by the arc, and the welding combined with the loss of the contact material causes the contact failure. While the final failure mode of the contact depends on the loss rate of the material and the severity of the fusion welding. The contact will fail at first due to the wear of the surface material if the material loss rate is fast and contact bonding failure may occur if welding is more severe.

Acknowledgment

The authors are grateful to the anonymous reviewers, and the editor, for their critical and constructive review of the manuscript. This study was co-supported by the National Natural Science Foundation of China (51507074, 61801196); Natural Science Foundation of Higher Education Institutions of Jiangsu Province (17KJB510014); Jiangsu Provincial Postgraduate Research and Practice Innovation Program Funding Project and Jiangsu Government Scholarship for Overseas Studies (JS-2018-260, JS-2018-259). Jiangsu Provincial Graduate Research and Practice Innovation Program Funding Project (KYCX19-1692).

References

1. Allen S E, Streicher E. The effect of microstructure on the electrical performance of Ag-WC-C contact materials. Proceedings of the 44th IEEE Holm Conference on Electrical Contacts 1998: 276-285.
2. Chen Z K, Witter G. Dynamic welding of silver contacts under different mechanical bounce condition. Proceedings of 45th IEEE Holm Conference on Electrical Contacts 1999: 1-8, <https://doi.org/10.1109/HOLM.1999.795920>.
3. Chen Z K, Witter G. Electrical contacts for automotive applications: a review. IEICE Transactions on Electronics 2004; E87-C (8): 1248-1254.
4. Chen Z K, Witter G. The effect of silver composition and additives on switching characteristics of silver tin oxide type contacts for automotive inductive load. Proceedings of the 51st IEEE Holm Conference on Electrical Contacts 2005: 35-41.
5. Leung C, Streicher E, Fitzgerald D, et al. Contact erosion of $AgSnO_2In_2O_3$ made by internal oxidation and powder metallurgy. Proceedings of the 51st IEEE Holm Conference on Electrical Contacts 2005: 22-27.
6. Liu D, Li Z B, Li C, et al. Experimental study on electromechanical characteristics of electrical contact in making and breaking operations. Low Voltage Apparatus 2013; 7(11): 10-14.

7. Liu D X, Li P Y, Rong M Z. Development of the equipment for electrical contact performance measurement. *Precious Metals* 2005; 26(4): 44-48.
8. Miyanaga K, Kayano Y, Komakine T, et al. effect of heat conductivity on bridge break at different material contact pairs. *IEICE Transactions on Electronics* 2011; E94-C(9): 1431-1434, <https://doi.org/10.1587/transele.E94.C.1431>.
9. Ning Y T, Zhao H Z. *Silver*. Changsha: Central South University Press, 2005.
10. Ren W B, Chen Y, Wang Z B, et al. Electrical contact resistance of coated spherical contacts. *IEEE Transactions on Electron Devices* 2016; 63(11): 4373-4379, <https://doi.org/10.1109/TED.2016.2612545>.
11. Ren W B, Du Y W, Man S D. A test rig for simulating the electrical performance of contact materials used in ac contactor. *Electrical & Energy Management Technology* 2016; (7): 11-15.
12. Ren W B, Jin J B, Li D, et al. Design and application of a novel test rig for simulating and evaluating electric arc and electrical contact characteristics of contact materials. *Electrical Materials* 2014; 4(7): 28-37.
13. Rong M Z, Li P Y, Li D X. The development of a new-type electrical contact performance measurement system of contacts. *Electrical Engineering Materials* 2005; (1): 17-21.
14. Rong M Z, Sun M. Study on surface dynamics characteristics of silver metal oxide (AgMeo) contact materials. *Chinese Society for Electrical Engineering* 1993; 13(6): 28-30.
15. Wang S B, Xie M, Liu M M, et al. Research progress of AgNi contact materials. *Rare Metal Materials and Engineering* 2013; 42(04): 875-880.
16. Wang S J, Yu Q. Study on contact failure mechanisms of accelerated life test for relay reliability. *IEICE Transactions on electronics* 2009; E92-C (8): 1034-1039, <https://doi.org/10.1587/transele.E92.C.1034>.
17. Wang S J, Yu Q, Zhai G F. The discrimination of contact failure mechanisms by analyzing the variations of time parameters for relays. *IEICE Transactions on Electronics* 2010; E93-C (9): 1437-1442, <https://doi.org/10.1587/transele.E93.C.1437>.
18. Wang, Z B, Shang S, Wang J W, et al. Accelerated storage degradation testing and failure mechanisms of aerospace electromagnetic relay. *Eksploatacja i Niezawodność - Maintenance and Reliability* 2017; 19(4): 530-541, <https://doi.org/10.17531/ein.2017.4.6>.
19. Zhou L K, Man S D, Wang Z B, et al. On the relationship between contact a-spots features and electrodynamic repulsion force for electrical apparatus. *IEEE Transactions on Components Packaging and Manufacturing Technology* 2018; 8(11): 1888-1895, <https://doi.org/10.1109/TCPMT.2018.2869993>.

ZhaoBin WANG**Shang SHANG**

School of Electronics and Information
Jiangsu University of Science and Technology
No. 02 Mengxi Street, Jingkou District
Zhenjiang, Jiangsu, 212003, P.R. China

School of Electronic and Electrical Engineering
University of Leeds
Leeds, LS2 9JT, United Kingdom

WeiYan LI**Zhan WANG****ChunYang HAN**

School of Electronics and Information
Jiangsu University of Science and Technology
No. 02 Mengxi Street, Jingkou District
Zhenjiang, Jiangsu, 212003, P.R.China

E-mails: wangzb@just.edu.cn, 1825339708@qq.com,
shangshang@just.edu.cn, 1165308663@qq.com,
605877761@qq.com, 1900562778@qq.com, 2358313772@qq.com
